Synthesis and Characterization of Two PET Radioligands for the Metabotropic Glutamate 1 (mGlu1) Receptor

YIYUN HUANG,[1,2]* RAJESH NARENDRAN,[1] FRANCOIS BISCHOFF,[3] NINGNING GUO,[1] SUNG A. BAE,[1] DAH-REN HWANG,[1,2] ANNE S. LESAGE,[4] AND MARC LARUELLE[1,2]

[1]*Department of Psychiatry, Columbia University College of Physicians and Surgeons, New York, New York*
[2]*Department of Radiology, Columbia University College of Physicians and Surgeons, New York, New York*
[3]*Department of Medicinal Chemistry, Johnson & Johnson Pharmaceutical Research and Development, A Division of Janssen Pharmaceutica, N.V., Beerse, Belgium*
[4]*CNS Discovery Research, Johnson & Johnson Pharmaceutical Research and Development, A Division of Janssen Pharmaceutica, N.V., Beerse, Belgium*

KEY WORDS Metabotropic glutamate receptor; Radioligand; Synthesis

ABSTRACT The metabotropic glutamate 1 receptor (mGlu1) is an important protein in the regulation of glutamate transmission in the brain, and believed to be involved in disorders such as ischemia, epilepsy, neuropathic pain, anxiety, and schizophrenia. The goal of this study was to evaluate two selective mGlu1 antagonists [^{11}C]**3** and [^{18}F]**4** as potential PET radioligands for the in vivo imaging of the mGlu1 receptor. Biodistribution studies in rats indicated high uptake of [^{11}C]**3** and [^{18}F]**4** in the brain. The highest activity level was found in the cerebellum, followed by striatum, hippocampus, frontal cortex, and medulla, in a pattern consistent with the distribution of mGlu1 receptor in rat. At 30 min postinjection, the activity ratio of cerebellum to medulla was 4.5 for [^{11}C]**3**, indicating a high degree of specific binding, while specific binding was lower for [^{18}F]**4** (cerebellum to medulla activity ratio of 2.0). Moreover, binding of the radioligands [^{11}C]**3** and [^{18}F]**4** in mGlu1 receptor-rich region such as cerebellum was blocked by pretreatment of the rats with their respective unlabeled compound or the selective mGlu1 antagonist (compound **5**, 2 mg/kg each), but not by the selective mGlu2 antagonist LY341495, or the selective mGlu5 antagonist MPEP (2 mg/kg), thus indicating the binding specificity and selectivity of [^{11}C]**3** and [^{18}F]**4** to the mGlu1 receptor. However, in imaging experiments in baboons [^{11}C]**3** displayed a small specific binding signal only in the cerebellum, while the specific binding of [^{18}F]**4** was difficult to detect. Species differences in receptor density and affinity of the radioligands in large part account for the differences in the behavior of [^{11}C]**3** and [^{18}F]**4** in rats and baboons. Radioligands with higher affinity and/or lower lipophilicity are needed to successfully image the mGlu1 receptor in humans. **Synapse 66:1002–1014, 2012.**

INTRODUCTION

The metabotropic glutamate receptors (mGlu) are G-protein-coupled receptors in the central nervous system that regulate cell excitability and synaptic transmission (Conn and Pin, 1997). They are classified into three major groups with eight subtypes (Group I: mGlu1 and 5; Group II: mGlu2 and 3; Group III: mGlu4, 6, 7, and 8) based on their sequence homology, signal transduction mechanism, and pharmacology (Pin and Acher, 2002). The Group I metabotropic receptors, which encompass the mGlu1 and 5 subtypes, are mainly postsynaptic receptors and have been implicated in disorders such as ischemia, epilepsy, neuropathic pain, anxiety, and schizophrenia (Bordi and Ugolini, 1999; Conn, 2003; Moghaddam, 2004). Therefore, the Group I metabotropic receptors have been the targets of intensive drug development effort (Conn, 2003; Spooren et al., 2003).

Contract grant sponsors: Johnson and Johnson Pharmaceutical Research and Development, A Division of Janssen Pharmaceutica, N.V., Beerse, Belgium

*Correspondence to: Yiyun Huang, PO Box 208048, PET Center, Department of Diagnostic Radiology, Yale University School of Medicine, 801 Howard Avenue, New Haven, CT 06520-8048, USA. E-mail: henry.huang@yale.edu

Received 20 June 2012; Accepted 20 August 2012

DOI 10.1002/syn.21606

Published online 28 August 2012 in Wiley Online Library (wileyonlinelibrary.com).

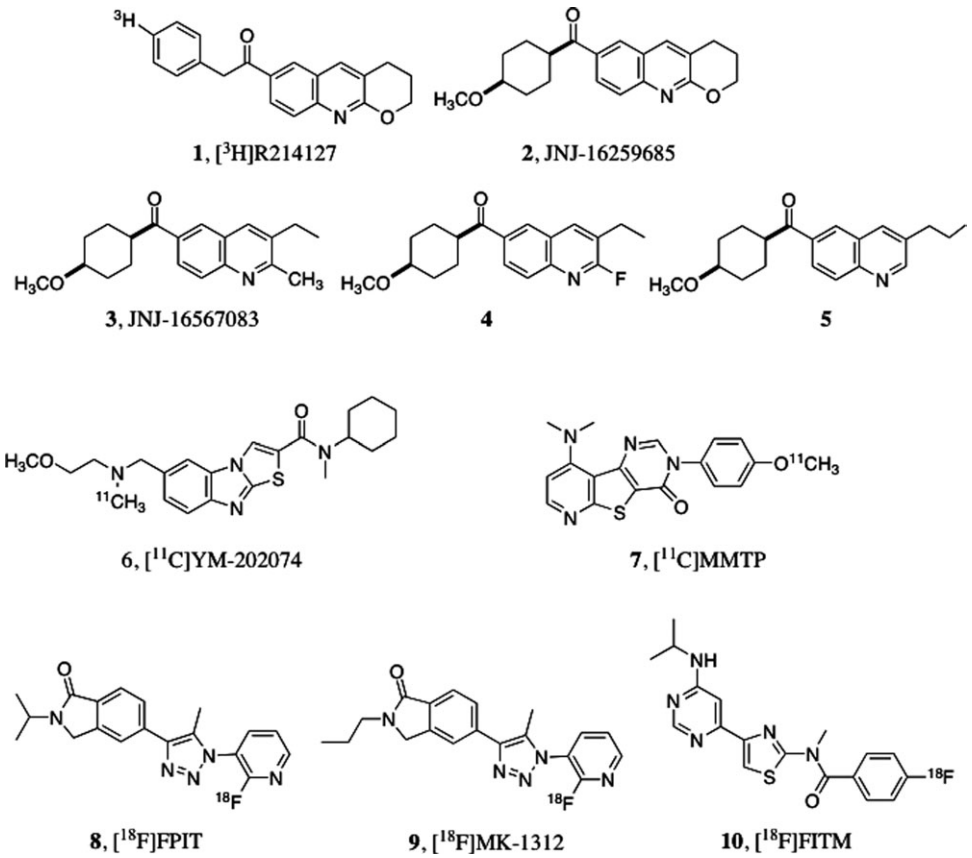

Fig. 1. Chemical structures of mGlu1 ligands and radioligands.

Over the years understanding of the mGlu5 receptor and its involvement in neurological and psychiatric disorders have been greatly advanced by the discovery of MPEP as a selective mGlu5 antagonist (Gasparini et al., 1999; Spooren et al., 2001). The emergence of selective radioligands such as [^{3}H]M-MPEP, [^{3}H]methoxymethyl-MTEP and [^{3}H]methoxy-PEPy then provided in vitro pharmacological tools to aid in the elucidation of mGlu5 functions (Cosford et al., 2003a,b; Gasparini et al.). Further, the recent discovery and application of positron emission tomography (PET) radiotracers such as [^{18}F]F-MTEP, [^{18}F]FPEB, and [^{11}C]ABP688 made it possible to quantitate mGlu5 receptor in vivo and to measure receptor occupancy of mGlu5 receptor targeting drugs (for reviews, see (Mu et al., 2010; Yu, 2007)). On the other hand, detailed study of mGlu1 receptor has been long hindered by the lack of selective ligands and radioligands for this receptor subtype. In 2005, Mabire et al. first described the synthesis and pharmacological evaluation of a series of quinoline derivatives as selective mGlu1 antagonists (Fig. 1) (Mabire et al., 2005), while Lavreysen et al. (2003, 2004a) reported the characterization of [^{3}H]R214127, also a quinoline derivative (Fig. 1), as a selective antagonist radioligand for mGlu1 receptor, which allows for the in vitro autoradiography and ex vivo labeling of the mGlu1 receptor. Results from pharmacological experiments also demonstrated the central activity of some compounds from these quinoline derivatives and indicated that compounds such as **2** (JNJ-16259685) and **3** (JNJ-16567083) possess anxiolytic-like properties in animal models after systemic administration (Lavreysen et al., 2004b; Pietraszek et al., 2005; Steckler et al., 2005). As a result, we identified two antagonist ligands (compounds **3** and **4**, Fig. 1) from this series for development as PET radioligands for the mGlu1 receptor. In a rapid communication, we reported the synthesis and preliminary evaluation of [^{11}C]**3** ([^{11}C]JNJ-16567083) in rodents (Huang et al., 2005). More recently, there have been renewed efforts in the development of PET radiotracers for mGlu1 receptor, owing to the emergence of new classes of selective mGlu1 antagonists, as exemplified by ligands **6–10** (Fig. 1) (Fujinaga et al., 2011, 2012a,b; Hostetler et al., 2011; Prabhakaran et al., 2010; Satoh et al., 2009; Yamasaki et al., 2010, 2011, 2012). This prompted us to disclose the comprehensive characterization of ligands [^{11}C]**3** and [^{18}F]**4** in rodents and nonhuman primates to assess their potential as PET radiotracers for imaging the mGlu1 receptor in vivo.

MATERIALS AND METHODS

Radiochemistry

Instruments used for radiochemistry are as follows: a semipreparative HPLC system including a Waters 515 HPLC pump (Waters, Milford, MA), a Rheodyne 7010 injector with a 2-mL loop, a Prodigy ODS-Prep C18 column (10 μm, 10 mm × 250 mm) (Phenomenex, Torrance, CA), an Alltech Model 450 UV detector, a custom-made gamma detector, and a PC running Look-Out HPLC data acquisition software; an analytical HPLC system consisting of a Waters 515 HPLC pump, a Rheodyne 7125 injector, a Phenomenex Prodigy ODS-3 C18 column (5 μm, 4.6 mm × 250 mm), a Waters PDA 996 detector, a flow cell gamma detector (Bioscan, Washington, DC), and a computer with the Empower software used for system control. [^{11}C]CO_2 was produced in a Siemens RDS-112 cyclotron with the bombardment of a nitrogen target with a proton source. Aqueous [^{18}F]NaF was produced via the (p, n) nuclear reaction of [^{18}O]H_2O. Irradiation of the target for 60 min usually generated >1000 mCi of radioactivity.

Synthesis of (3-ethyl-2-[^{18}F]fluoro-6-quinolinyl)((1s,4s)-4-methoxycyclohexyl) methanone ([^{18}F]4)

Aqueous [^{18}F]NaF was mixed with K_2CO_3 and Kryptofix 222 in a 5-mL reaction vial. Water was removed by repeated addition of anhydrous MeCN and azeotropic evaporation of the resulting mixture to bring the [^{18}F]fluoride to complete dryness and ready for use in fluorination reaction.

The precursor **11** (2 mg) in DMSO (1 mL) was added to the reaction vial containing anhydrous [^{18}F]fluoride. The mixture was heated at 150°C for 5 min, cooled, and diluted with water (50 mL). The resulting aqueous solution was passed through a C18 SepPak and the SepPak rinsed with 25% aqueous MeOH (20 mL). The crude product, eluted off the SepPak with EtOH (1 mL), was then purified by preparative HPLC (mobile phase: 50%MeCN/50% 0.1 M ammonium formate; flow rate: 8 mL/min). The product fraction, eluted off the column at ~24 min, was collected, diluted with water (100 mL) and passed through a C18 SepPak. The SepPak was rinsed with 0.01 N HCl (10 mL) and H_2O (10 mL). The final product was eluted off the SepPak with EtOH (1 mL), and formulated by dilution of the EtOH solution with sterile normal saline (9 mL) and filtration of the solution through a sterile membrane filter (0.22 μm). Radiochemical purity of the final product was >98%. Average radiochemical yield was 27% (decay-corrected, n = 6). Average specific activity was 1.067 Ci/μmol at end of synthesis (n = 6). Total synthesis time was about 80 min. Identity of the labeled compound [^{18}F]**4** was confirmed by co-injection of the product in saline with the unlabeled compound **4** onto the analytical HPLC (mobile phase: 65% MeCN/35% 0.1 M ammonium formate; flow rate: 2 mL/min). The radiolabeled product and the unlabeled compound **4** co-eluted from the column, and only one single UV peak (t_R = 7.6 min) was detected.

In vitro binding assays

Membrane preparation from dihydrofolate reductase-deficient Chinese hamster ovary (CHO-dhfr$^-$) cells expressing the rat mGlu1a receptors

CHO-dhfr$^-$ cells stably expressing rat mGlu1a receptor were a gift from S. Nakanishi (Tokyo University, Tokyo, Japan). Cells were grown in Dulbecco's modified Eagle's medium with GlutaMAX I supplemented with 10% heat-inactivated fetal calf serum, 0.4 mM L-proline, 0.2 mg/mL streptomycin sulfate, and 200 U/mL penicillin. Cells were kept in an atmosphere of 37°C and 5% CO_2. Confluent cells were washed in ice-cold phosphate-buffered saline and stored at −20°C until membrane preparation. After thawing, cells were suspended in 50 mM Tris-HCl, pH 7.4, and collected through centrifugation for 10 min at 23,500 g at 4°C. The cells were lysed in 10 mM hypotonic Tris-HCl, pH 7.4. After centrifugation for 20 min at 30,000 g at 4°C, the pellet was homogenized with an Ultra Turrax homogenizer in 50 mM Tris-HCl, pH 7.4. Protein concentrations were measured by the Bio-Rad protein assay using bovine serum albumin as standard.

Radioligand binding to rat mGlu1a receptor CHO-dhf$^-$ membranes at 4°C

[^{3}H]R214127 binding (Lavreysen et al., 2003). After thawing, the membranes were homogenized using an Ultra Turrax homogenizer and suspended in ice-cold binding buffer containing 50 mM Tris-HCl, pH 7.4, 1.2 mM $MgCl_2$, and 2 mM $CaCl_2$, unless otherwise indicated. Ligand saturation experiments were performed at apparent binding equilibrium (30 min of incubation) with 20 μg of membrane protein and 10 concentrations (0.1, 0.2, 0.3, 0.4, 0.5, 1, 2, 2.5, 5, and 10 nM) of the radioligand. Nonspecific binding was estimated in the presence of 1 μM of R193845. The incubation was stopped by rapid filtration under suction over GF/C glass-fiber filters using a manual 40-well filtration manifold. The filters were transferred to scintillation vials and, after the addition of Ultima-Gold MV, the radioactivity collected on the filters was counted in a Packard scintillation counter. For inhibition experiments, assay mixtures were incubated for 30 min at 4°C in a volume of 0.5 mL containing 20–40 μg of membrane protein, appropriate concentrations of the test compound and 2.5 nM [^{3}H]R214127. Nonspecific binding was defined as earlier. Filtration

was performed using Unifilter-96 GF/C filter plates and a 96-well PerkinElmer filtermate harvester. After the addition of microscint O, radioactivity on the filters was counted in the Microplate scintillation and luminescence counter.

[^{3}H]R214127 binding to rat cerebellum membranes at 37°C in physiological buffer

Tissue preparation. Male Wistar rats (~200 g) were sacrificed by decapitation. The brains were rapidly removed and the cerebellum was dissected. The fresh tissue was homogenized with an Ultra Turrax in 20 volumes of 50 mM Tris-HCl, pH 7.4, and tissue was centrifuged at 23,500 g for 10 min. After homogenization using a DUALL homogenizer, membranes were washed twice by centrifugation at 23,500 g for 10 min. The final pellet was suspended in 10 volumes of 50 mM Tris-HCl, pH 7.4, and frozen at −80 °C.

In vitro binding assay. After thawing, membranes from rat cerebellum were homogenized using a DUALL homogenizer and suspended in ice-cold binding buffer containing 1.25 mM $NaHPO_4$, 15 mM $NaHCO_3$, 10 mM *D*-glucose, 128 mM NaCl, 3 mM KCl, 2 mM $CaCl_2$, and 2 mM $MgSO_4$, pH 7.5. The binding assay was carried out in a total volume of 0.5 mL containing 2.5 nM [^{3}H]R214127 and a membrane aliquot corresponding to 40 μg of cerebellar membranes. Specific binding was calculated as the difference between the total binding and the binding measured in the presence of 1 μM R193845. After incubation for 30 min at 37°C, the labeled membranes were washed and harvested by rapid vacuum filtration over Whatman GF/C glass-fiber filters using a 40-well filtration manifold, and radioactivity collected on the filters was counted as above.

Measurement of partition coefficient

Measurement of partition coefficient followed the published procedure, with some modifications (Wilson et al., 2001). Briefly, 0.2–0.4 mCi of the radioligand was added to a separatory funnel containing *n*-octanol (20 mL) and 0.02 M phosphate buffer (pH 7.4, 20 mL). The mixture was shaken mechanically for 3 min and the layers were separated. The aqueous layer was discarded. The *n*-octanol layer (15 mL) was transferred to a second separatory funnel containing 15 mL of the phosphate buffer (pH 7.4). The mixture was shaken mechanically for 3 min and the layers were separated. The aqueous layer was discarded and the *n*-octanol layer was then partitioned into four test tubes (2 mL of the octanol solution each) containing 2 mL of the phosphate buffer each. The test tubes were vortexed for 10 min, and then centrifuged for 10 min at 1000 g to separate the layers. The *n*-octanol and aqueous phases (1.0 mL each) were transferred into counting tubes and counted with a gamma counter. The radioactivity counts were decay-corrected and the partition coefficient calculated as follows: P = counts in *n*-octanol/counts in buffer. Reported log P value represents the mean of 4 separate calculations.

Biodistribution studies in rats

Biodistribution experiments in rats were performed according to protocols approved by the New York State Psychiatric Institute/Columbia University Institutional Animal Care and Use Committee (IACUC). For each set of experiment, the labeled compound [^{11}C]**3** or [^{18}F]**4** in saline was injected into groups of male Sprague-Dawley rats (3 rats for each group) via the tail vein and the rats were sacrificed by decapitation, following inhalation of CO_2, at 10, 30, 60, and 90 min after radioactivity injection. The brain regions (cerebellum, hippocampus, striatum, frontal cortex, and medulla), along with samples of blood and part of the tail, were removed, weighed, and counted in a Packard Cobra II gamma counter (Packard, Meriden, CT). The percent injected dose (%ID) of the decay- and tail-corrected activity in the brain regions and blood were calculated based upon C-11 standards prepared from the same radioligand solution, and the %ID/g calculated using the tissue weights. In another set of experiments, four groups of rats (three rats in each group) were treated with the unlabeled compound **3** or **4**, compound **5** (selective mGlu1 antagonist), LY341495 (selective mGlu2 antagonist), or MPEP (selective mGlu5 antagonist) (2 mg/kg each, iv) 10–15 min before the radiotracer injection. In a control group rats (n = 3) were injected with saline. Each group of rats was sacrificed 30 min after the injection of the radioactivity. Blood sample and brain tissues were taken, counted, weighed and %ID/g calculated based on decay-corrected counts. The average %ID/g in the control group was then compared with that from each of the pretreatment groups.

PET imaging in baboon

Imaging protocol

PET imaging experiments in baboons were performed according to protocol approved by the Columbia-Presbyterian Medical Center Institutional Animal Care and Use Committee. Fasted animals were immobilized with ketamine (10 mg/kg, i.m.) and anesthetized with 1.8% isoflurane via an endotracheal tube. Vital signs were monitored every 10 min and the temperature was kept constant at 37°C with heated water blankets. An i.v. perfusion line was used for hydration and injection of radiotracers. A catheter was inserted in a femoral artery for arterial blood sampling. The head of the baboon was positioned at the center of the field of view as defined by imbedded laser lines. PET

scans were performed with the ECAT EXACT HR+ PET camera (Siemens, Knoxville, TN). A 15-min transmission scan was obtained prior to radiotracer injection. Radioactivity was injected i.v. in 30 s. Emission data were collected in the 3D mode for 90 min as 21 successive frames of increasing duration (6 × 10 s, 2 × 1 min, 4 × 2 min, 2 × 5 min, 7 (10) × 10 min).

Input function measurement

Arterial blood samples were collected every 10 s with an automated system for the first 2 min, every 20 s between 2 and 4 min, and manually thereafter at various intervals. A total of 28 samples were collected. Following centrifugation (10 min at 1800 g), the plasma was collected and activity was measured in a 200-μL aliquot on a gamma counter (Wallac 1480 Wizard 3M Automatic Gamma Counter, Perkin-Elmer, Waltham, MA).

Metabolite analysis

Additional blood samples were taken at 2, 4, 12, 30, 60, and 90 min after radioactivity injection for analysis of metabolites and the parent compound. After centrifugation the plasma was separated and transferred to a tube containing 1 mL of MeOH. The mixture was vortexed and centrifuged at 15,000 g for 5 min to separate the pellet from the aqueous phase. The supernatant was then taken up in a syringe and injected onto an HPLC column and analyzed (Phenomenex Prodigy C18 ODS-3 column, 10 μm, 4.6 mm × 250 mm; mobile phase: 60%MeCN/40% 0.1 M ammonium acetate for analysis of ligand [^{11}C]**3** and 65%MeCN/35% 0.1 M ammonium formate for [^{18}F]**4**; flow rate: 2 mL/min; retention times for the parent compounds [^{11}C]**3** and [^{18}F]**4**: ~8 min). Fractions were collected, counted and decay-corrected to calculate the percentage of the parent compound in the blood at different time points. Before plasma sample analysis, the retention time of the parent compound was established by injection of a small amount of the radioligand solution and detection of the radioactivity peak using a Bioscan gamma detector. The arterial input function was corrected for the presence of metabolites as previously described (Abi-Dargham et al., 1999), and used for kinetic analysis of brain uptake. The clearance of the parent compound (C_L, L/h) was calculated as the ratio of the injected dose to the area under the curve of the input function (Abi-Dargham et al., 1994; Rowland and Tozer, 1989).

Free fraction measurement

For the determination of the plasma free fraction (f_p), triplicate 200 μL aliquots of plasma (separated from blood collected prior to tracer injection) were mixed with the radiotracer and pipetted into ultrafiltration units (Centrifree, Amicon, Danvers, MA) and centrifuged at room temperature (20 min at 4000 rpm) (Gandelman et al., 1994). Plasma and ultrafiltrate activities were counted, and f_p was calculated as the ratio of the ultrafiltrate activity to the total plasma activity. Triplicate aliquots of the radiotracer in Tris buffer (pH 7.4) were also processed to determine the filter retention of free tracer.

Image analysis

Image analysis was performed as previously described (Abi-Dargham et al., 1999). Briefly, a magnetic resonance image (MRI) of each baboon's brain was obtained for the purpose of identifying the regions of interest (ROI) (T1-weighted axial MRI sequence, acquired parallel to the anterior–posterior commissure, TR 34 ms, TE 5 ms, flip angle of 45°, slice thickness is 1.5 mm, zero gap, matrix 1.5 mm × 1 mm × 1 mm voxels). PET emission data were attenuation-corrected using the transmission scan, and frames were reconstructed using a Shepp filter (cutoff 0.5 cycles/projection rays). Reconstructed image files were then processed by the image analysis software MEDx (Sensor Systems, Sterling, VA). Frames were summed. The summed image was used to define the registration parameters with the MR image, using between-modality automated image registration (AIR) algorithm (Woods et al., 1993), and individual frames were registered to the MR data set. The following regions of interest (ROIs) were drawn on the MR images: cerebellum, striatum, hippocampus, cingulate cortex, occipital cortex, and medulla. Regions were transferred to the registered PET frames, and time–activity curves were measured and decay-corrected. Right and left regions were averaged.

Derivation of distribution volume (V_T)

Regional total distribution volumes (V_T, in mL/g) were derived by kinetic analysis of the regional time–activity curves, using the metabolite-corrected arterial plasma concentrations as the input function, according to a one- or two-tissue-compartment model. Kinetic parameters (K_1 and k_2 for the one-tissue-compartment model; K_1–k_4 for the two-tissue-compartment model) were derived first in modeling analysis. In the one-tissue-compartment model, K_1 (mL/min/g) and k_2 (min^{-1}) are the rate constants governing the transfer of the ligands into and out of the brain, respectively. In the two-tissue-compartment model, K_1 and k_2 are the rate constants governing the transfer of the ligands into and out of the nondisplaceable compartment (free and nonspecific binding), whereas k_3 (min^{-1}) and k_4 (min^{-1}) describe the respective rates of association to and dissociation from the receptors.

V_T was derived from kinetic parameters as $V_T = K_1/k_2$ in the one-tissue compartment model, and as $V_T = K_1/k_2\,(1 + k_3/k_4)$ in the two-tissue compartment model.

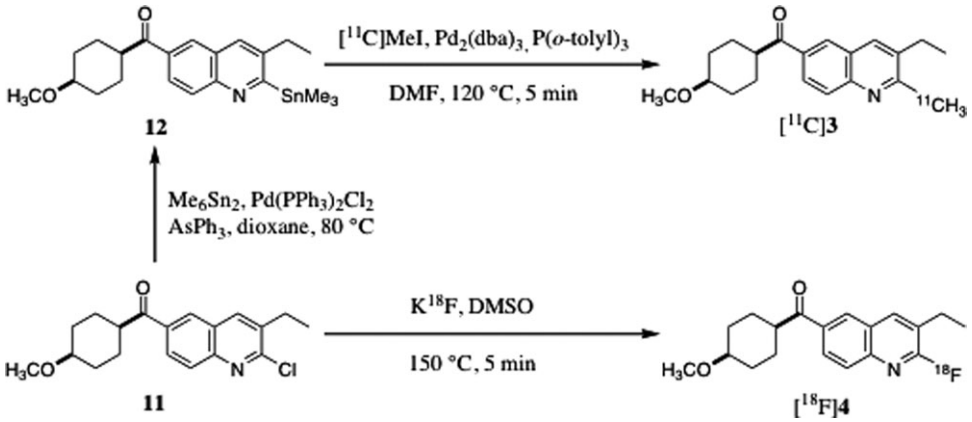

Fig. 2. Synthesis of the radiolabeled mGlu1 antagonists [^{11}C]**3** and [^{18}F]**4**.

*TABLE 1. In vitro binding affinities of ligands **3** and **4***[a]

	*K*i (nM)								
	Cloned rat mGlu1a receptor			Rat cerebellar membranes			Cloned human mGlu1 receptor		
Compound	4°C	37°C	Ratio (37°C/4°C)	4°C	37°C	Ratio (37°C/4°C)	4°C	37°C	Ratio (37°C/4°C)
3	0.87 ± 0.43	3.49 ± 0.93	4.0	0.57 ± 0.41	4.41 ± 1.59	7.7	4.75 ± 0.70	13.3 ± 6.49	2.8
4	0.87 ± 0.14	3.38 ± 1.66	3.9	1.07 ± 0.38	1.77 ± 1.01	1.7	3.74 ± 1.31	24.7 ± 6.32	6.6

[a]Data presented are mean ± SD of four separate determinations.

RESULTS

Chemistry and radiochemistry

Synthesis of the radioligands [^{11}C]**3** and [^{18}F]**4** is depicted in Figure 2. Preparation of Compounds **3**, **4,** and **11** as the fluorine-18 labeling precursor followed the literature procedures (Mabire et al., 2005). Reaction of compound **11** with hexamethylditin under Pd-catalyzed conditions gave the C-11 labeling precursor **12** in 41% yield and radiolabeling with [^{11}C]MeI produced [^{11}C]**3** in 47% radiochemical yield and >99% radiochemical purity, as previously reported (Huang et al., 2005).

Preparation of tracer [^{18}F]**4** was accomplished by nucleophilic substitution of compound **11** with [^{18}F]KF in DMSO at 150°C. The radiosynthesis gave both the *cis*- and *trans*-isomers in a 40/60 ratio. Semipreparative HPLC separated the two isomers (t_R = 21 min for the *trans*-isomer and 24 min for the *cis*-isomer). The desired *cis*-isomer (compound [^{18}F]**4**) was isolated in 27% average radiochemical yield (n = 6, decay-corrected). Radiochemical purity of the final product was >98%. Total synthesis time was about 80 min. Average specific activity was 1,067 Ci/μmol at EOS (n = 6). Identity of the labeled compound was confirmed by co-injection of the product [^{18}F]**4** with the unlabeled compound **4** and observation of a single UV peak on the analytical HPLC chromatogram.

Partition coefficient measurement

Measurement of partition coefficient followed a modified version of the published procedures. The log *P* of the radioligands [^{11}C]**3** and [^{18}F]**4** was determined to be 3.38 ± 0.11 and 3.54 ± 0.14, respectively (n = 4 measurements each), indicating that ligand [^{18}F]**4** has slightly higher lipophilicity than [^{11}C]**3**.

In vitro binding affinity

The affinities of compounds **3** and **4** for mGlu1 receptor were assayed in vitro using cloned rat mGlu1a receptor stably expressed on CHO cells, cloned human mGlu1 receptor stably expressed on HEK cells, and rat cerebellum membranes, respectively. Measurements were performed at 4°C and at 37°C in physiological buffer. Results are listed in Table I. At 4°C, both compounds display high affinities for the cloned rat mGlu1a receptor and rat cerebellum membranes (*K*i of 0.87 ± 0.43 nM and 0.87 ± 0.14 for cloned rat mGlu1a receptor, and 0.57 ± 0.41 nM and 1.07 ± 0.38 nM for rat cerebellar membranes, respectively, for compounds **3** and **4**), while their affinities for the cloned human mGlu1 receptor were slightly lower (*K*i of 4.75 ± 0.70 and 3.74 ± 1.31 nM, respectively, for Compounds **3** and **4**). At 37°C and under physiological conditions, the binding affinities of compounds **3** and **4** are generally lower than

*TABLE II. Distribution of radioligands [^{11}C]**3** and [^{18}F]**4** in male Sprague-Dawley rats*[a]

		Brain region					
Time	Blood	Medulla	Cerebellum	Striatum	Hippocampus	Frontal cortex	Specific binding (cerebellum)
[^{11}C]**3**							
10 min	0.41 ± 0.01	0.46 ± 0.04	1.15 ± 0.18	0.71 ± 0.09	0.57 ± 0.09	0.54 ± 0.11	2.48 ± 0.35
30 min	0.29 ± 0.07	0.15 ± 0.02	0.66 ± 0.06	0.19 ± 0.03	0.19 ± 0.03	0.14 ± 0.03	4.53 ± 0.55
60 min	0.20 ± 0.04	0.09 ± 0.04	0.31 ± 0.08	0.11 ± 0.02	0.09 ± 0.03	0.09 ± 0.03	3.86 ± 0.89
[^{18}F]**4**							
10 min	0.16 ± 0.04	0.41 ± 0.14	0.70 ± 0.23	0.43 ± 0.14	0.36 ± 0.12	0.33 ± 0.09	1.72 ± 0.15
30 min	0.15 ± 0.06	0.18 ± 0.05	0.37 ± 0.11	0.18 ± 0.06	0.16 ± 0.05	0.14 ± 0.03	2.03 ± 0.22
60 min	0.07 ± 0.01	0.07 ± 0.01	0.12 ± 0.02	0.07 ± 0.00	0.06 ± 0.01	0.06 ± 0.01	1.66 ± 0.28
90 min	0.06 ± 0.01	0.06 ± 0.02	0.08 ± 0.03	0.06 ± 0.02	0.05 ± 0.01	0.06 ± 0.03	1.42 ± 0.17

[a]Uptake in the blood and brain regions is expressed as % injected dose per gram of tissue (% ID/g); Specific binding is expressed as the ratio of activity in the region of interest to that in the medulla. Values for [^{11}C]**3** are mean ± SD of six animals in each group, while those for [^{18}F]**4** are mean ± SD of three animals in each group.

*TABLE III. Distribution of radioligands [^{11}C]**3** and [^{18}F]**4** in rats under control and pretreatment conditions*[a]

		Brain region					
Condition	Blood	Medulla	Cerebellum	Striatum	Hippocampus	Frontal cortex	Specific binding (cerebellum)
[^{11}C]**3**							
Control	0.27 ± 0.08	0.16 ± 0.01	0.68 ± 0.05	0.30 ± 0.09	0.23 ± 0.04	0.26 ± 0.08	4.12 ± 0.25
3	0.29 ± 0.06	0.13 ± 0.03	0.13 ± 0.03	0.14 ± 0.03	0.11 ± 0.02	0.12 ± 0.03	1.04 ± 0.28
5	0.27 ± 0.02	0.15 ± 0.06	0.13 ± 0.03	0.15 ± 0.05	0.11 ± 0.03	0.12 ± 0.05	0.93 ± 0.21
LY341495	0.31 ± 0.07	0.18 ± 0.02	0.69 ± 0.11	0.40 ± 0.11	0.31 ± 0.09	0.26 ± 0.07	3.89 ± 0.52
MPEP	0.26 ± 0.03	0.18 ± 0.04	0.69 ± 0.07	0.28 ± 0.10	0.24 ± 0.09	0.22 ± 0.07	3.86 ± 0.54
[^{18}F]**4**							
Control	0.11 ± 0.01	0.14 ± 0.01	0.29 ± 0.06	0.14 ± 0.02	0.13 ± 0.02	0.11 ± 0.02	2.01 ± 0.33
4	0.10 ± 0.01	0.15 ± 0.01	0.16 ± 0.02	0.15 ± 0.02	0.13 ± 0.03	0.13 ± 0.03	1.10 ± 0.18
5	0.08 ± 0.01	0.12 ± 0.01	0.10 ± 0.01	0.11 ± 0.02	0.10 ± 0.02	0.10 ± 0.01	0.87 ± 0.07
MPEP	0.08 ± 0.01	0.16 ± 0.02	0.32 ± 0.04	0.19 ± 0.02	0.15 ± 0.03	0.14 ± 0.01	1.97 ± 0.21

[a]Uptake in the blood and brain regions is expressed as % injected dose per gram of tissue (% ID/g); Specific binding is expressed as the ratio of activity in the region of interest to that in the medulla. Rats in the control group were treated with saline 10 min before radioligand injection, while those in the pre-treatment groups were injected with the unlabeled compounds (**3** or **4**), compound **5**, LY341495 or MPEP (2 mg/kg each, given i.v. 10 min before tracer). Animals were sacrificed 30 min after radioligand injection. Values are mean ± SD of three to nine animals in each group.

those measured at 4°C, demonstrating a significant effect of temperature on binding affinity (Table I). Also noteworthy is the differences in binding affinities between the cloned rat and human mGlu1 receptors, with both compounds displaying at least four times lower affinity for human than rat mGlu1 receptor under various assay conditions.

Biodistribution in rats

The results from ex vivo biodistribution studies in male Sprague-Dawley rats are listed in Table II. For ligand [^{11}C]**3**, the initial uptake in the brain was high, with ID/g in various brain regions ranging from 0.46% in the frontal cortex to 1.15% in the cerebellum at 10 min after radioligand injection, thus indicating an excellent entry of the radioligand into the brain. Over time, radioactivity was highly concentrated in the cerebellum, where the level of mGlu1 receptor is high. Using the medulla, where the density of mGlu1 receptor is the lowest (Lavreysen et al., 2004a), as the reference region, the ratio of radioactivity in the region of interest to that in the medulla, which can be used as a measure of specific binding, was 4.53 for the cerebellum at 30 min postinjection. There are some indication of specific binding in other brain regions as well (ratio $>$ 1), including the striatum and hippocampus.

For ligand [^{18}F]**4**, both brain uptake and specific binding in the cerebellum were lower than those of [^{11}C]**3**. Peak uptake was 0.70 % ID/g in the cerebellum at 10 min postinjection. Peak-specific binding in the cerebellum was 2.01 at 30 min postinjection (Table II).

To test the binding specificity and selectivity of the radioligands in the rat brain, groups of rats were injected with the unlabeled compound, the selective mGlu1 antagonist **5**, the mGlu2 antagonist LY341495 (Kingston et al., 1998), or the selective mGlu5 antagonist MPEP (Gasparini et al., 1999) before injection of the radiotracer. When the rats were pretreated with the unlabeled compound **3** or the selective mGlu1 antagonist **5**, regional uptake and specific binding of [^{11}C]**3** were significantly reduced. For example, uptake in the cerebellum was reduced by 81% by both compounds **3** and **5**, and specific binding decreased by 75 and 77%, respectively, by compounds **3** and **5** (Table III). On the other hand, pretreatment of the animals with the selective mGlu2 antagonist LY341495 or mGlu5 antagonist MPEP produced no significant changes in either the regional uptake or

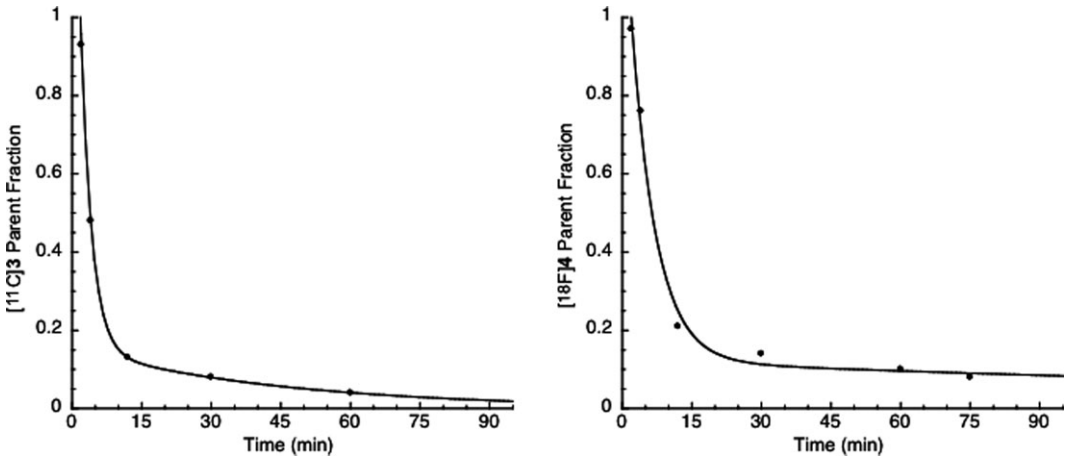

Fig. 3. Plot of parent fraction in the plasma over time for the radiotracers [^{11}C]**3** (left panel) and [^{18}F]**4** (right panel). Metabolism of both radioligands is rapid, with less than 20% of the radioactivity in the plasma corresponding to the parent fraction at 15 min postinjection. Overall, radioligand [^{11}C]**3** displays a significantly faster metabolism than [^{18}F]**4**.

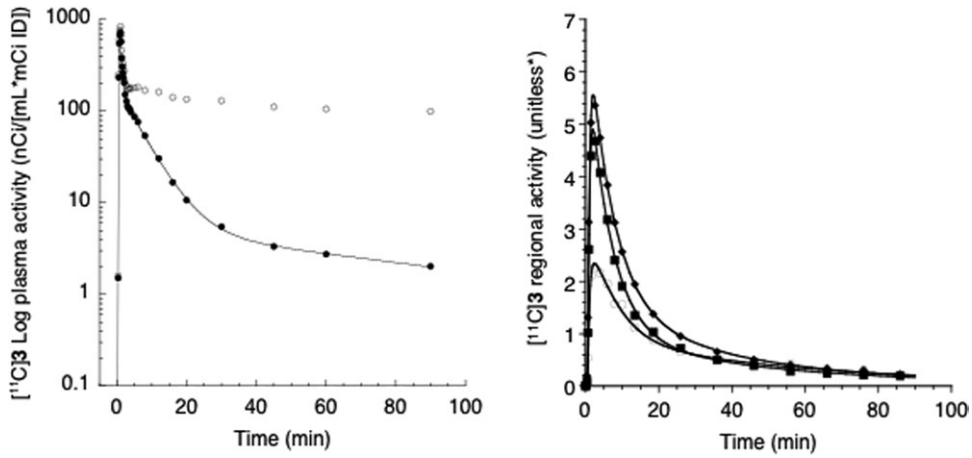

Fig. 4. Time–activity curves of the radiotracer [^{11}C]**3** in the plasma (left panel) and brain (right panel) of a baboon. In the left panel, data represent total (open circles) and metabolite-corrected (closed circles) plasma parent activities in log scale. Lines are data fitted to two exponentials. In the right panel, points are activities measured in the cerebellum (closed diamond), striatum (closed squares), and medulla (open circles). Lines are values fitted by a two-tissue (2T) compartment model. Activity concentrations are normalized by the injected dose and body weight (kg). Rapid brain uptake is observed, followed by a rapid clearance. There appears to be observable, but small differences in the regional uptake of [^{11}C]**3**, indicating a small degree of specific binding in mGlu1-rich regions (cerebellum and striatum).

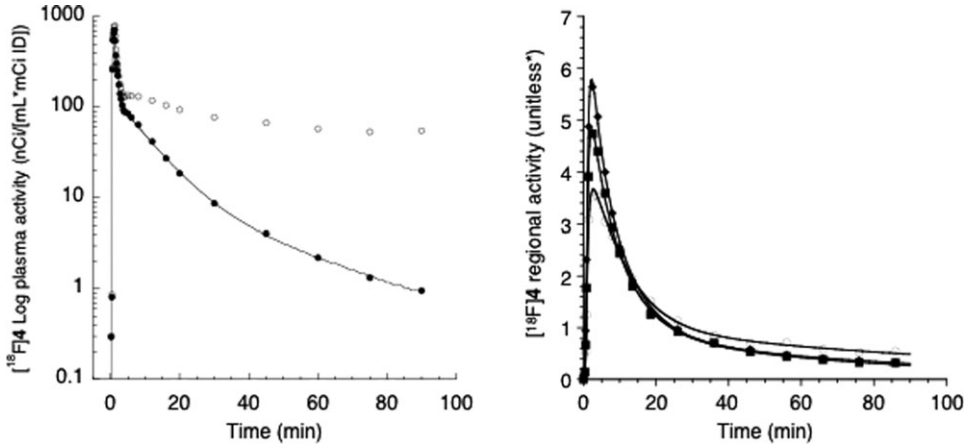

Fig. 5. Time–activity curves of the radiotracer [^{18}F]**4** in the plasma (left panel) and brain (right panel) of a baboon. In the left panel, data represent total (open circles) and metabolite-corrected (closed circles) plasma parent activities in log scale. Lines are data fitted to two exponentials. In the right panel, points are activities measured in the cerebellum (closed diamond), striatum (closed squares), and medulla (open circles). Lines are values fitted by a two-tissue (2T) compartment model. Activity concentrations are normalized by the injected dose and body weight (kg). Rapid brain uptake is observed, followed by a rapid clearance. There appears to be little observable differences in the regional uptake of [^{18}F]**4**.

*TABLE IV. Lipophilicity (log P), plasma free fraction (f_P), plasma clearance rate (L/h), and brain regional distribution volume (V_T mL/g) of radioligands [^{11}C]**3** and [^{18}F]**4** in baboons*[a]

Ligand	Log *P*	f_p	Clearance	Regional V_T					
				Medulla	Cerebellum	Striatum	Hippocampus	Cingulate cortex	Occipital cortex
[^{11}C]**3**	3.38 ± 0.11	1.4 ± 0.3%	40.6 ± 2.4	2.4 ± 12.5	2.9 ± 0.3	2.2 ± 0.2	2.5 ± 0.2	2.4 ± 0.2	2.3 ± 0.2
[^{18}F]**4**	3.54 ± 0.14	0.6%	36.6	3.7	2.9	2.5	2.9	2.9	3.2

[a]Values of f_P, plasma clearance rate, and brain regional V_T are mean ± SD of five measurements in four baboons for [^{11}C]**3** and one measurement for [^{18}F]**4**.

specific binding of [^{11}C]**3** in any of the brain regions examined (Table III).

Similar drug effects were observed with the radioligand [^{18}F]**4**. When the rats were pretreated with the unlabeled compound **4** or the selective mGlu1 antagonist **5**, uptake in the cerebellum was decreased by 44% and 64%, respectively, and specific binding by 45% and 57% (Table III). In addition, pretreatment with MPEP induced no significant changes in the uptake or specific binding of [^{18}F]**4**. Taken together, ex vivo experiments in rats indicated that the PET radioligands [^{11}C]**3** and [^{18}F]**4** displayed adequate brain uptake, and their binding in the brain is saturable, specific and selective to the mGlu1 receptor. Overall, specific binding of [^{11}C]**3** is higher than that of [^{18}F]**4**.

PET imaging experiments in baboons

Results from PET imaging experiments in baboons were shown in Figures 3–5 and Table IV. Injected dose was 4.1 ± 0.5 mCi for [^{11}C]**3** (n = 5) and 1.6 mCi for [^{18}F]**4** (n = 1).

Plasma analysis

Both radioligands [^{11}C]**3** and [^{18}F]**4** bind avidly to the plasma protein, with protein-bound fraction of the ligands at > 98%. Free fraction (f_P) in the plasma was 1.4% ± 0.3% for [^{11}C]**3** (n = 5) and 0.6% for [^{18}F]**4** (n = 1). In addition, [^{11}C]**3** and [^{18}F]**4** were rapidly metabolized into more polar components in the blood. At 12 min postinjection, only about 13% of the total activity in the plasma corresponded to the parent compound [^{11}C]**3**, and this number decreased to 8 and 4%, respectively, at 30 and 60 min postinjection (Fig. 3, left panel). For [^{18}F]**4**, parent fraction in the plasma was 21, 14, 8%, respectively, at 12, 30, and 60 min postinjection (Fig. 3, right panel). Metabolism of [^{11}C]**3** is significantly faster than [^{18}F]**4**.

Plasma activity displayed an initial distribution phase after radioligand injection, which increased rapidly, reached a peak and then decreased thereafter (Figs. 4 and 5, left panels). The log *P* values, plasma free fraction, plasma clearance rate, and regional distribution volumes of [^{11}C]**3** and [^{18}F]**4** are provided in Table IV. For [^{11}C]**3** and [^{18}F]**4**, plasma clearance rates were 40.5 ± 12.5 L/h (n = 5) and 36.6 L/h (n = 1), respectively. There was no significant difference in plasma clearance between [^{11}C]**3** and [^{18}F]**4**.

Brain analysis

Radioactivity distributed rapidly into the baboon brain, and also cleared quickly a few minutes after injection. Peak uptake was reached at about 2 min after injection of [^{11}C]**3** or [^{18}F]**4** (Figs. 4 and 5, right panels). For [^{11}C]**3**, there were small differences in uptake levels among brain regions, with higher activity levels in the cerebellum and striatum compared to that in the medulla, indicating a small but detectable specific binding in the cerebellum and striatum. For [^{18}F]**4**, there were no discernable differences in regional uptake.

Regional distribution volumes for [^{11}C]**3** and [^{18}F]**4** are listed in Table IV. Kinetic modeling analysis using the two-tissue compartment (2T) model confirmed a small but detectable regional specific binding for radioligand [^{11}C]**3**. The cerebellum, where the density of mGlu1 is the highest, displays the highest distribution volume (V_T) of 2.9 ± 0.3 mL/g (n = 5). Value of V_T in the medulla was 2.4 ± 0.4 mL/g (n = 5). Distribution volumes in other brain areas were similar to that in the medulla (Table IV). The specific binding signal in the cerebellum was confirmed in a blocking experiment, as co-injection of the radioligand with 2 mg/kg of the unlabeled compound **3** reduced cerebellum V_T by 60%, while V_T values in other brain regions were not affected. Overall, kinetic analysis indicated a small degree of specific binding for [^{11}C]**3** in the cerebellum only, with negligible specific binding signals in other brain regions of the baboon. For [^{18}F]**4**, modeling analysis confirmed the lack of specific binding in any of the baboon brain regions. Distribution volumes in all regions of interest were lower than that in the medulla (Table IV).

DISCUSSSION

The PET radioligands [^{11}C]**3** and [^{18}F]**4** were prepared in high specific activity and high radiochemical purity. Results from ex vivo distribution studies in rats indicated that [^{11}C]**3** displayed relatively high specific binding to the mGlu1 receptor, while the specific binding of [^{18}F]**4** was lower. We have previous

reported that MicroPET imaging experiment in a living rat confirmed the specific binding of [^{11}C]**3** to the mGlu1 receptor in vivo (Huang et al., 2005). However, in PET imaging experiments in baboons radioligand [^{11}C]**3** displayed a small specific binding signal in the cerebellum only, while [^{18}F]**4** failed to provided detectable specific binding signals. Several factors may have contributed to the differences in the binding characteristics of these two radioligands between rats and baboons.

Effect of temperature on binding affinities

Examination of the binding data listed in Table I reveals a significant effect of temperature on the binding affinities of ligands **3** and **4**. For example, there was a four-fold decrease in the binding affinities of ligands **3** and **4** to the cloned rat mGlu1 receptor when temperature was raised from 4 to 37°C. These same decreases were also observed for binding to the rat cerebellar membrane and cloned human mGlu1 receptor. In the literature, similar temperature effect on the binding affinities to the serotonin transporter has been noted for most, but not all selective serotonin reuptake inhibitors (SSRIs) (Elfving et al., 2001). We have also reported previously the effect of temperature on the binding affinity of fallypride to the dopamine D_2 receptor (Slifstein et al., 2004). In addition, Laruelle et al. (1994a,b) observed the same temperature effect on the binding affinities of another D_2 ligand IBF and the benzodiazepine ligand iomazenil.

In vivo K_d

As noted earlier, temperature sometimes exerts an effect on the binding affinities of radioligands (Elfving et al., 2001). Since the in vivo binding of a radioligand occurs at body temperature (37°C), the in vivo K_d may be different from those measured in vitro either at reduced (4°C) or room (22°C) temperature. For example, the binding affinity of fallypride for the dopamine D_2 receptor in the rat striatum was 0.04 nM at 22°C and 2.03 nM at 37 °C, while the in vivo K_d derived from imaging experiments with [^{18}F]fallypride in baboons was 0.2 nM in the striatum (Slifstein et al., 2004). For the other D_2 ligand IBF, the in vivo K_d (0.081 nM for [^{123}I]IBF) was between the K_i's measured in vitro at 22°C (0.06 nM) and 37°C (0.10 nM) (Laruelle et al., 1994b). The benzodiazepine receptor ligand iomazenil is another case in which the in vivo K_d (0.54 nM for [^{123}I]iomazenil) derived from imaging experiments fell between those measured in vitro at 22°C (0.35 nM) and 37°C (0.66 nM) (Laruelle et al., 1994a). It should be noted that the differences between in vivo and in vitro K_d may not be significant enough for IBF and iomazenil. The point is that sometime there is significant temperature effect on the binding affinity of a radioligand, hence the binding affinities of perspective PET radioligands at body temperature (37°C) should be assessed to better correlate the in vitro and in vivo behavior.

Binding affinities to the rat mGlu1 receptor

At 4°C, the binding affinities of the two ligands **3** and **4** to the cloned rat mGlu1 receptor and the mGlu1 receptor in the rat cerebellum are high, with K_i's of <1 nM (Table I). Binding affinities measured at body temperature and under physiological conditions are slightly lower, but still in the low nanomolar range (K_i's of 1.8–4.4 nM, respectively). On the basis of the analyses presented earlier, it is reasonable to propose that the in vivo K_d for the rat mGlu1 receptor is between 0.57 and 4.41 nM for ligand **3**, and between 0.87 and 3.38 nM for ligand **4**. These binding affinities appear to be sufficiently high to provide a degree of specific binding in vivo in rats (Table I). As both ligands display similar binding affinities to the rat mGlu1 receptor, the lower free fraction in the blood and slightly higher lipophilicity associated with the radioligand [^{18}F]**4** (Table IV) may have contributed to its lower brain uptake (peak cerebellum uptake of 1.15 % ID/g for [^{11}C]**3** vs 0.70% ID/g for [^{18}F]**4** at 10 min after injection) and lower specific binding in rats (peak specific binding in the cerebellum of 4.5 for [^{11}C]**3** vs 2.0 for [^{18}F]**4** at 30 min post-injection) (Table II).

Binding affinities to the human mGlu1 receptor

The binding affinities of compounds **3** and **4** to the cloned human mGlu1 receptor are markedly lower than those to their rat counterpart. At 4 °C, the K_i's of ligands **3** and **4** for the human mGlu1 receptor are 4.75 and 3.74 nM, respectively, vs 0.87 nM and 0.87 nM for the cloned rat mGlu1 receptor. At 37 °C and under physiological conditions, ligands **3** and **4** display K_i's of 13.3 and 24.7 nM, respectively, for the human mGlu1 vs 3.49 and 3.38 nM for the cloned rat mGlu1 receptor.

Assuming that the binding affinities of ligands **3** and **4** to the baboon mGlu1 receptor are similar to those to its human counterpart and the in vivo K_d's are somewhere between those measured at 4°C and 37°C, then the in vivo K_d for the baboon mGlu1 receptor should be between 4.75 and 13.3 nM for ligand **3** and between 3.74 and 24.7 nM for ligand **4**. These values are at least four times higher than those for the rat mGlu1 receptor, indicating that the binding affinities of these two ligands are at least four times lower going from rat to baboon. This species difference in binding affinities may in large part account for the fact that radioligands [^{11}C]**3** and [^{18}F]**4** provide noticeable specific binding in rats, but barely observable specific binding signals for ligand [^{11}C]**3** and negligible specific binding signals for [^{18}F]**4** in baboons.

TABLE V. Concentrations (B_{max}) of mGlu1 receptor in regions of rat, monkey, and human brain

	Regional B_{max} (nM)			
Species	Cortex	Hippocampus	Striatum	Cerebellum
Rat[a]	47.1 ± 6.8	68.8 ± 12.5	74.1 ± 4.8	430.2 ± 204.2
Rhesus monkey[b]	10 ± 1.9	–	–	53 ± 12
Human[b]	26 ± 15	–	–	82 ± 33 24.7 ± 6.32 6.6

[a]From Lavreysen et al., 2004a.
[b]From Hostetler et al., 2011.

Receptor distribution in rat and baboon

Another factor that may have contributed to the different behavior of the radioligands is the differences in receptor distribution in rat and baboon. In rat, quantitative autoradiography studies have demonstrated that the mGlu1 receptor distribution in the brain follows a gradient, with the highest concentration in the cerebellum, followed by the striatum, hippocampus, cortex, and with the lowest concentration in the medulla (Lavreysen et al., 2004a; Mutel et al., 2000). It has been noted that the relative abundance of mGlu1 receptor in the human brain followed the same rank order (Mutel et al., 2000). Recently, Hostetler et al. (2001) reported the mGlu1 receptor concentrations in the cerebellum and cortex of rhesus monkeys and humans from quantitative analysis of saturation binding experiments. Literature values of B_{max} from rat, monkey and human are summarized in Table V. As expected, regional B_{max} values in rhesus monkeys are at least five times lower than those in rats. Assuming the same regional mGlu1 distribution and concentrations between rhesus monkeys and baboons, it is not surprising, then, that specific binding signals provided by radioligand [^{11}C]**3**, which is proportional to B_{max}/K_d, decreased dramatically from rat to baboon. Hence, the results presented in this paper indicate that the species difference in binding affinities and receptor densities in large part accounts for the discrepancies in the in vivo behavior of the radioligands [^{11}C]**3** and [^{18}F]**4** in rat and baboon.

Summary and future directions

Results from this study indicate that radioligands [^{11}C]**3** and [^{18}F]**4** displayed specific binding in ex vivo experiments in rats. We have previously reported that in vivo imaging of the mGlu1 receptor in rat can be achieved using the radioligand [^{11}C]**3** and PET (Huang et al., 2005). However, data presented in this report demonstrate that reliable quantification of the same receptor with [^{11}C]**3** or [^{18}F]**4** is not possible in nonhuman primates, and by extension, in humans. The relatively low binding affinity of radioligand [^{11}C]**3** and [^{18}F]**4** to the human mGlu1 receptor, especially at body temperature, as well as the lower density of mGlu1 receptor in large part account for this failure of [^{11}C]**3** and [^{18}F]**4** in the higher species. Another contributing factor might be the ligand's relatively high lipophilicity, which results in low free fraction in the plasma and high nonspecific binding in the brain. On the basis of these analyses, we concluded that successful ligand development for PET imaging of the human mGlu1 receptor should be focused on the discovery of high affinity mGlu1 ligands with lower lipophilicity, and that owing to species difference in mGlu1 receptor expression, assessment of a tracer's suitability for in vivo imaging should be conducted in nonhuman primates as soon as possible. Recent efforts in mGlu1 PET ligand development confirm these points. For example, [^{11}C]YM-202074 (**6**) and [^{11}C]MMTP (**7**) (Fig. 1), with K_i of 4.8 and 7.9 nM for cloned human mGlu1 receptor and Log P of 2.7 and 3.15, respectively, displayed low brain uptake and little specific binding signals in vivo (Prabhakaran et al., 2010; Yanamoto et al., 2010). Ligand [^{18}F]FPIT (**8**, Fig. **1**), with an IC_{50} of 5.4 nM for cloned human mGlu1 receptor and lipophilicity of 2.53, showed good specific binding signals in rats, with peak cerebellum to medulla ratio of 4.27, similar to what we found with [^{11}C]**3** (Fujinaga et al., 2012a). However, specific binding in the monkey brain was much reduced, with peak cerebellum to pons ratio of only 1.62. Along with the results presented in this report, findings with [^{18}F]FPIT further confirm significant species differences in tracer behavior, and thus underscore the importance of assessing a ligand's true potential in imaging mGlu1 receptors in vivo in higher species as soon as possible. Up to date, two mGlu1 radioligands, [^{18}F]MK-1312 (**9**) and [^{18}F]FITM (**10**) (Fig. 1), have been found to provide adequate specific binding signals in regions of the monkey brain (Hostetler et al., 2011; Yamasaki et al., 2011, 2012). These two radioligands share some favorable properties: (1) optimal lipophilicity, with Log P of 2.3 and 1.5 for [^{18}F]MK-1312 and [^{18}F]FITM, respectively, which should lead to lower nonspecific binding in the monkey brain; (2) higher affinity, with IC_{50} of 3.6 and 5.1 nM, respectively, for cloned human mGlu1 receptor. Since mGlu1 receptor B_{max} in the human cerebellum and cortex appears to be higher than rhesus monkeys (Table V) (Hostetler et al., 2011), it is reasonable to postulate that [^{18}F]MK-1312 and [^{18}F]FITM will be able to provide measurable specific binding signals in humans for the quantification of mGlu1 receptors.

CONCLUSION

The radioligands [^{11}C]**3** and [^{18}F]**4** were successfully prepared in high specific activity and high radiochemical purity. Evaluation of these two radioligands for their ability to label the mGlu1 receptor in vivo has

been carried out in rats and baboons. In ex-vivo biodistribution studies in rats, [^{11}C]**3** and [^{18}F]**4** displays specific and selective binding to the mGlu1 receptor in the cerebellum, striatum, and hippocampus. Previous report of MicroPET imaging experiment in rat also confirms the specific binding of [^{11}C]**3** to the mGlu1 receptor in vivo. On the other hand, results from PET imaging experiments in baboons indicate that the radioligand [^{11}C]**3** displays small but detectable specific binding in the baboon brain, while specific binding of [^{18}F]**4** is not detectable. Species difference in binding affinities (i.e., decrease from rat to human mGlu1 receptor) and their changes with temperature (i.e., decrease from 4 to 37°C) contribute to the discrepancies in the behavior of these two radioligands in rats and baboons. Given the potential effect of temperature and that PET imaging is performed at body temperature, it is important to determine the binding affinities of candidate PET radioligands at different temperatures (e.g., at 4 and 37 °C) to assess their true potential to image the target receptor in vivo. From the findings in the present study we conclude that development of successful PET radioligands to image the mGlu1 receptor in nonhuman primates and humans requires the discovery of compounds with higher affinity and lower lipophilicity. Such compounds are emerging, and recent efforts in this area have produced candidate PET radioligands that hold promise in imaging mGlu1 receptors in humans. The availability of such PET imaging agents will aid in the further understanding of this receptor subtype in neuropsychiatric disorders.

ACKNOWLEDGMENTS

We thank the expert technical assistance of Elizabeth Hackett, John Castrillon, Lyudmilla Savenkova, and Nosirudeen Quadri.

REFERENCES

Abi-Dargham A, Laruelle M, Seibyl J, Rattner Z, Baldwin RM, Zoghbi SS, Zea-Ponce Y, Bremner JD, Hyde TM, Charney DS, Hoffer PB, Innis RB. 1994. SPECT measurement of benzodiazepine receptors in human brain with [^{123}I]iomazenil: Kinetic and equilibrium paradigms. J Nucl Med 35:228–238.

Abi-Dargham A, Simpson N, Kegeles L, Parsey R, Hwang DR, Anjilvel S, Zea-Ponce Y, Lombardo I, Van Heertum R, Mann JJ, Foged C, Halldin C, Laruelle M. 1999. PET studies of binding competition between endogenous dopamine and the D_1 radiotracer [^{11}C]NNC 756. Synapse 32:93–109.

Bordi F, Ugolini A. 1999. Group I metabotropic glutamate receptors: Implications for brain diseases. Prog Neurobiol 59:55–79.

Conn PJ. 2003. Physiological roles and therapeutic potential of metabotropic glutamate receptors. Ann N Y Acad Sci 1003:12–21.

Conn PJ, Pin JP. 1997. Pharmacology and functions of metabotropic glutamate receptors. Annu Rev Pharmacol Toxicol 37: 205–237.

Cosford ND, Roppe J, Tehrani L, Schweiger EJ, Seiders TJ, Chaudary A, Rao S, Varney MA. 2003a. [^{3}H]-Methoxymethyl-MTEP and [^{3}H]-Methoxy-PEPy: Potent and selective radioligands for the metabotropic glutamate subtype 5 (mGlu5) receptor. Bioorg Med Chem Lett 13:351–354.

Cosford ND, Tehrani L, Roppe J, Schweiger E, Smith ND, Anderson J, Bristow L, Brodkin J, Jiang X, McDonald I, Rao S, Washburn M, Varney MA. 2003b. 3-[(2-Methyl-1,3-thiazol-4-yl)ethynyl]-pyridine: A potent and highly selective metabotropic glutamate subtype 5 receptor antagonist with anxiolytic activity. J Med Chem 46:204–206.

Elfving B, Bjornholm B, Ebert B, Knudsen GM. 2001. Binding characteristics of selective serotonin reuptake inhibitors with relation to emission tomography studies. Synapse 41:203–211.

Fujinaga M, Yamasaki T, Kawamura K, Kumata K, Hatori A, Yui J, Yanamoto K, Yoshida Y, Ogawa M, Nengaki N, Maeda J, Fukumura T, Zhang MR. 2011. Synthesis and evaluation of 6-[1-(2-[^{18}F]fluoro-3-pyridyl)-5-methyl-*1H*-1,2,3-triazol-4-yl]quinoline for positron emission tomography imaging of the metabotropic glutamate receptor type 1 in brain. Bioorg Med Chem 19:102–110.

Fujinaga M, Maeda J, Yui J, Hatori A, Yamasaki T, Kawamura K, Kumata K, Yoshida Y, Nagai Y, Higuchi M, Suhara T, Fukumura T, Zhang MR. 2012a. Characterization of 1-(2-[^{18}F]fluoro-3-pyridyl)-4-(2-isopropyl-1-oxo-isoindoline-5-yl)-5-methyl-*1H*-1,2,3-triazole, a PET ligand for imaging the metabotropic glutamate receptor type 1 in rat and monkey brains. J Neurochem 121:115–124.

Fujinaga M, Yamasaki T, Yui J, Hatori A, Xie L, Kawamura K, Asagawa C, Kumata K, Yoshida Y, Ogawa M, Nengaki N, Fukumura T, Zhang MR. 2012b. Synthesis and evaluation of novel radioligands for positron emission tomography imaging of metabotropic glutamate receptor subtype 1 (mGluR1) in rodent brain. J Med Chem 55:2342–2352.

Gandelman MS, Baldwin RM, Zoghbi SS, Zea-Ponce Y, Innis RB. 1994. Evaluation of ultrafiltration for the free fraction determination of single photon emission computerized tomography (SPECT) radiotracers: β-CIT, IBF and iomazenil. J Pharmaceutical Sci 83:1014–1019.

Gasparini F, Andres H, Flor PJ, Heinrich M, Inderbitzin W, Lingenhohl K, Muller H, Munk VC, Omilusik K, Stierlin C, Stoehr N, Vranesic I, Kuhn R. 2002. [^{3}H]-M-MPEP, a potent, subtype-selective radioligand for the metabotropic glutamate receptor subtype 5. Bioorg Med Chem Lett 12:407–409.

Gasparini F, Lingenhohl K, Stoehr N, Flor PJ, Heinrich M, Vranesic I, Biollaz M, Allgeier H, Heckendorn R, Urwyler S, Varney MA, Johnson EC, Hess SD, Rao SP, Sacaan AI, Santori EM, Velicelebi G, Kuhn R. 1999. 2-Methyl-6-(phenylethynyl)-pyridine (MPEP), a potent, selective and systemically active mGlu5 receptor antagonist. Neuropharmacology 38:1493–1503.

Hostetler ED, Eng W, Joshi AD, Sanabria-Bohorquez S, Kawamoto H, Ito S, O'Malley S, Krause S, Ryan C, Patel S, Williams M, Riffel K, Suzuki G, Ozaki S, Ohta H, Cook J, Burns HD, Hargreaves R. 2011. Synthesis, characterization, and monkey PET studies of [^{18}F]MK-1312, a PET tracer for quantification of mGluR1 receptor occupancy by MK-5435. Synapse 65:125–135.

Huang Y, Narendran R, Bischoff F, Guo N, Zhu Z, Bae SA, Lesage AS, Laruelle M. 2005. A positron emission tomography radioligand for the *in vivo* labeling of metabotropic glutamate 1 receptor: (3-ethyl-2-[^{11}C]methyl-6-quinolinyl)(*cis*-4-methoxycyclohexyl)methanone. J Med Chem 48:5096–5099.

Kingston AE, Ornstein PL, Wright RA, Johnson BG, Mayne NG, Burnett JP, Belagaje R, Wu S, Schoepp DD. 1998. LY341495 is a nanomolar potent and selective antagonist of group II metabotropic glutamate receptors. Neuropharmacology 37:1–12.

Laruelle M, Abi-Dargham A, al-Tikriti MS, Baldwin RM, Zea-Ponce Y, Zoghbi SS, Charney DS, Hoffer PB, Innis RB. 1994a. SPECT quantification of [^{123}I]iomazenil binding to benzodiazepine receptors in nonhuman primates. II. Equilibrium analysis of constant infusion experiments and correlation with *in vitro* parameters. J Cereb Blood Flow Metab 14:453–465.

Laruelle M, Al-Tikriti MS, Zea-Ponce Y, Zoghbi SS, Baldwin RM, Charney DS, Hoffer PB, Kung HF, Innis RB. 1994b. In vivo quantification of dopamine D_2 receptors parameters in nonhuman primates with [^{123}I]iodobenzofuran and single photon emission computerized tomography. Eur J Pharmacol 263:39–51.

Lavreysen H, Janssen C, Bischoff F, Langlois X, Leysen JE, Lesage AS. 2003. [^{3}H]R214127: A novel high-affinity radioligand for the mGlu1 receptor reveals a common binding site shared by multiple allosteric antagonists. Mol Pharmacol 63:1082–1093.

Lavreysen H, Pereira SN, Leysen JE, Langlois X, Lesage AS. 2004a. Metabotropic glutamate 1 receptor distribution and occupancy in the rat brain: A quantitative autoradiographic study using [^{3}H]R214127. Neuropharmacology 46:609–619.

Lavreysen H, Wouters R, Bischoff F, Nobrega Pereira S, Langlois X, Blokland S, Somers M, Dillen L, Lesage AS. 2004b. JNJ16259685, a highly potent, selective and systemically active mGlu1 receptor antagonist. Neuropharmacology 47:961–972.

Mabire D, Coupa S, Adelinet C, Poncelet A, Simonnet Y, Venet M, Wouters R, Lesage AS, Van Beijsterveldt L, Bischoff F. 2005. Synthesis, structure-activity relationship, and receptor pharmacology of a new series of quinoline derivatives acting as selective, noncompetitive mGlu1 antagonists. J Med Chem 48:2134–2153.

Moghaddam B. 2004. Targeting metabotropic glutamate receptors for treatment of the cognitive symptoms of schizophrenia. Psychopharmacology (Berl) 174:39–44.

Mu L, Schubiger PA, Ametamey SM. 2010. Radioligands for the PET imaging of metabotropic glutamate receptor subtype 5 (mGluR5). Curr Top Med Chem 10:1558–1568.

Mutel V, Ellis GJ, Adam G, Chaboz S, Nilly A, Messer J, Bleuel Z, Metzler V, Malherbe P, Schlaeger EJ, Roughley BS, Faull RL, Richards JG. 2000. Characterization of [^{3}H]quisqualate binding to recombinant rat metabotropic glutamate 1a and 5a receptors and to rat and human brain sections. J Neurochem 75:2590–2601.

Pietraszek M, Sukhanov I, Maciejak P, Szyndler J, Gravius A, Wislowska A, Plaznik A, Bespalov AY, Danysz W. 2005. Anxiolytic-like effects of mGlu1 and mGlu5 receptor antagonists in rats. Eur J Pharmacol 514:25–34.

Pin JP, Acher F. 2002. The metabotropic glutamate receptors: Structure, activation mechanism and pharmacology. Curr Drug Target CNS Neurol Disord 1:297–317.

Prabhakaran J, Majo VJ, Milak MS, Kassir SA, Palner M, Savenkova L, Mali P, Arango V, Mann JJ, Parsey RV, Kumar JS. 2010. Synthesis, *in vitro* and *in vivo* evaluation of [^{11}C]MMTP: A potential PET ligand for mGluR1 receptors. Bioorg Med Chem Lett 20:3499–3501.

Rowland M, Tozer TN. 1989. Clinical pharmacokinetics. Philadelphia, PA: Lea & Febiger.

Satoh A, Nagatomi Y, Hirata Y, Ito S, Suzuki G, Kimura T, Maehara S, Hikichi H, Satow A, Hata M, Ohta H, Kawamoto H. 2009. Discovery and *in vitro* and *in vivo* profiles of 4-fluoro-*N*-[4-[6-(isopropylamino)pyrimidin-4-yl]-1,3-thiazol-2-yl]-*N*-methylbenzamide as novel class of an orally active metabotropic glutamate receptor 1 (mGluR1) antagonist. Bioorg Med Chem Lett 19:5464–5468.

Slifstein M, Hwang DR, Huang Y, Guo N, Sudo Y, Narendran R, Talbot P, Laruelle M. 2004. *In vivo* affinity of [^{18}F]fallypride for striatal and extrastriatal dopamine D_2 receptors in nonhuman primates. Psychopharmacology (Berl) 175:274–286.

Spooren W, Ballard T, Gasparini F, Amalric M, Mutel V, Schreiber R. 2003. Insight into the function of Group I and Group II metabotropic glutamate (mGlu) receptors: Behavioural characterization and implications for the treatment of CNS disorders. Behav Pharmacol 14:257–277.

Spooren WP, Gasparini F, Salt TE, Kuhn R. 2001. Novel allosteric antagonists shed light on mglu receptors and CNS disorders. Trends Pharmacol Sci 22:331–337.

Steckler T, Lavreysen H, Oliveira AM, Aerts N, Van Craenendonck H, Prickaerts J, Megens A, Lesage AS. 2005. Effects of mGlu1 receptor blockade on anxiety-related behaviour in the rat lick suppression test. Psychopharmacology (Berl) 179:198–206.

Wilson AA, Jin L, Garcia A, DaSilva JN, Houle S. 2001. An admonition when measuring the lipophilicity of radiotracers using counting techniques. Appl Radiat Isot 54:203–208.

Woods RP, Mazziotta JC, Cherry SR. 1993. MRI-PET registration with automated algorithm. J Comput Assist Tomogr 17:536–546.

Yamasaki T, Fujinaga M, Maeda J, Kawamura K, Yui J, Hatori A, Yoshida Y, Nagai Y, Tokunaga M, Higuchi M, Suhara T, Fukumura T, Zhang MR. 2012. Imaging for metabotropic glutamate receptor subtype 1 in rat and monkey brains using PET with [^{18}F]FITM. Eur J Nucl Med Mol Imaging 39:632–641.

Yamasaki T, Fujinaga M, Yoshida Y, Kumata K, Yui J, Kawamura K, Hatori A, Fukumura T, Zhang MR. 2011. Radiosynthesis and preliminary evaluation of 4-[^{18}F]fluoro-*N*-[4-[6-(isopropylamino)-pyrimidin-4-yl]-1,3-thiazol-2-yl]-*N*-methylbenzamide as a new positron emission tomography ligand for metabotropic glutamate receptor subtype 1. Bioorg Med Chem Lett 21:2998–3001.

Yanamoto K, Konno F, Odawara C, Yamasaki T, Kawamura K, Hatori A, Yui J, Wakizaka H, Nengaki N, Takei M, Zhang MR. 2010. Radiosynthesis and evaluation of [^{11}C]YM-202074 as a PET ligand for imaging the metabotropic glutamate receptor type 1. Nucl Med Biol 37:615–624.

Yu M. 2007. Recent developments of the PET imaging agents for metabotropic glutamate receptor subtype 5. Curr Top Med Chem 7:1800–1805.